Plug-flow anaerobic digestion with multi-position sensors

The value of gradient measurement for process monitoring

Longis, Marion; Pereira, Joana Carvalho; Högl, Thomas H.; Neubauer, Peter; Junne, Stefan

Published in:
Biomass and Bioenergy

DOI (link to publication from Publisher):
10.1016/j.biombioe.2023.106803

Publication date:
2023

Document Version
Publisher's PDF, also known as Version of record

Biomass and Bioenergy 173 (2023) 106803

Contents lists available at ScienceDirect

Biomass and Bioenergy

journal homepage: www.elsevier.com/locate/biombioe

Plug-flow anaerobic digestion with multi-position sensors: The value of gradient measurement for process monitoring

Marion Longis [a], Joana Carvalho Pereira [a], Thomas H. Högl [a], Peter Neubauer [a], Stefan Junne [a,b,*]

[a] Bioprocess Engineering, Institute of Biotechnology, Technische Universität Berlin, Ackerstrasse 76 ACK 24, D-13355, Berlin, Germany
[b] Department of Chemistry and Bioscience, Aalborg University Esbjerg, Niels Bohrs Vej 8, DK-6700, Esbjerg, Denmark

ARTICLE INFO

Keywords:
Plug-flow
Anaerobic digestion
Gradient formation
Acidification
Dark fermentation
On-line monitoring

ABSTRACT

In the present study, a tailor-made plug-flow reactor with 3D-printed parts and a multi-position monitoring of the pH-value, conductivity and ORP at the inlet, center and outlet part is introduced and applied in anaerobic digestion in order to investigate whether i) the formation of gradients can be detected, ii) ideal single or multiple spots for the location of sensors during an acidification process can be identified, and iii) the spatial gradient acquisition allows for an indirect monitoring of process performance measures, e.g. the accumulation of short-chain carboxylic acids.

During the acidification of a full digestion and in dark fermentation with maize and grass silage, the multi-position monitoring of the liquid phase revealed that the local monitoring of conductivity at the inlet and center, the ORP at the center and outlet and the pH-value at the outlet are relevant to gain information of the process performance, while the spatial gradient monitoring of the conductivity between the inlet and center and of the ORP between the center and outlet are relevant for the early detection of process disturbances.

1. Introduction

Any circular bioeconomy concept relies on the utilization of a wide range of biogenic residual feedstock. Biogenic residues, like agricultural side products or biowaste are regarded as valuable feedstock for AD. They are used more and more frequently for AD aside of composting [1,2]. AD consists of four major process phases: i) hydrolysis, ii) acidogenesis, iii) acetogenesis, and iv) methanogenesis. While fermentative bacteria are the main actors in the three primary phases, methanogenic organisms are the drivers of the final conversion of the organic intermediates into methane (CH_4) in the last phase of the process [3]. When the methanogenesis is suppressed, a so-called DF, or acidogenic mixed culture fermentation, is achieved, in which the carbon feedstock is converted, beside biomass, into hydrogen, ethanol, and SCCAs (e.g. acetic acid, butyric acid, propionic acid, a. o.) [4]. Biohydrogen production from biogenic waste through DF is a promising technology as biohydrogen is considered as a future energy carrier where, theoretically, 1 mol of glucose produces 4 mol of H_2 together with 2 mol of acetic acid [5]. Also, SCCAs are intensively used in the chemical industry as building blocks of alcohols, aldehydes, alkanes, esters and ketones. They can also be used as substrate to produce biofuels and biopolymers, namely PHAs [6]. Most recently, SCCAs from DF have been applied for the production of valuable polyunsaturated fatty acids like DHA and EPA in oleaginous microorganisms [7].

DF is a process mode that occurs, if, for example, an anaerobic mixed culture is acidified, like it can happen as process disturbance in full AD as well, although highly unwanted in the latter case. Process recovery takes usually weeks or months until the previous capacity for biogas production in full AD is achieved again. However, also a combination of these two operation modes, namely DF and AD, is possible, if several consecutive reactors or reactors with segregated zones are used. The utilization of a PFR proved to achieve a stable process for an increased efficiency at a high solid content of 20–30% DM, making it a favored system for the anaerobic digestion of the organic fraction of municipal waste for biogas production [8,9] While in CSTRs, all or at least several AD phases occur simultaneously everywhere in the vessel, the alternative configuration of a PFR allows for the segregation of the different phases of AD along the reactor. Thus, at a short HRT, hydrolytic and acidogenic reactions occur mainly near the feedstock input in the direction of the flow, while methanogenesis occurs at a longer HRT, in the second part of the reactor closer to the outlet. The sequential separation of AD phases along a PFR has been observed, for example, by Namsree

* Corresponding author. Department of Chemistry and Bioscience, Aalborg University Esbjerg, Niels Bohrs Vej 8, DK-6700, Esbjerg, Denmark.
E-mail addresses: stefan.junne@tu.berlin.de, sju@bio.aau.dk (S. Junne).

https://doi.org/10.1016/j.biombioe.2023.106803
Received 15 January 2023; Received in revised form 13 March 2023; Accepted 10 April 2023
Available online 20 April 2023

et al. [10]. In a PFR-based digestion of pineapple pulp and peel, acidogenic bacteria dominated near the entrance while methanogens dominated the microbial consortium in the central and final section of the PFR. The segregation of AD phases has also been observed in a PFR-based digestion of cheese whey, in which hydrolysis and acidogenesis were identified in the first part, whereas acetogenesis and methanogenesis occurred in the other parts of the reactor [11]. A gradient formation in *off-line* monitored parameters such as pH, FOS/TAC, sCOD has also been observed in co-digestion of swine manure and corn stover at an OLR of 4.7 $kg_{VS}m^{-3}d^{-1}$ and HRT of 28d for biogas production [12].

In many studies about PFR-based digestion, *off-line* measurements of the pH-value, alkalinity, SCCAs, TS and VS, as well as off-gas analysis have been typically performed with samples from ports that were arbitrarily located along the PFR. Although the separation of the different phases of AD should lead to a gradient formation along the reactor length, their formation has not been studied systematically yet. *On-line* monitoring in the liquid phase of AD typically covers parameters such as pH-value and temperature. Very rarely, the *on-line* and at least partly automated measurement of COD, TOC, SCCA concentration, alkalinity, turbidity and biogas composition has been reported [13]. Although numerous convenient technologies exist for the *on-line* monitoring of the liquid phase in anaerobic bioprocesses, e.g. as summarized by Bockisch *et al.* [14], they are often not applied in practice yet. This is surprising as some examples show promising results and potential for process control. The data correlate with parameters that describe the process performance, which otherwise require laborious *off-line* analyses: for instance, the ORP is known to be a crucial parameter to monitor the hydrolysis of waste sludge, while it correlates well with the soluble COD [15]. Additionally, a linear relation has been observed between *on-line* conductivity measurements and *off-line* measurements of SCCA concentrations up to 5 g L^{-1} [16,17], as well as bicarbonate concentrations and methane production rates in AD [18].

These examples provide a motivation for the utilization of sensors in the liquid phase of a PFR-based digestion process: the application of multi-position monitoring of parameters such as pH-value, ORP and conductivity, as well as the determination of their gradients along the HRT, may allow for the early identification of process disturbances like acidification or a lack of nutrients [19]. The consideration of spatial gradients instead of single one-spot measurements may provide even better estimations of the process performance and may be an important basis for process models. If so, multiposition measurements might be able to improve process control and a secured operation at flexible feedstock composition and load in a PFR.

In order to prove the authors' hypothesis, a multi-position monitoring approach has been applied to evaluate the performance of a digestion process, mainly operated under acidic conditions in a dark fermentation mode with real-time monitoring at the inlet, center, and outlet part of a PFR. In order to decrease costs, increase design flexibility and allow a fast implementation of reactors in any lab to conduct continuous experiments quickly with a broad range of feedstock, a PFR made out of 3D-printed and plexiglass material was designed for this study. 3D-printing is a rapid, easily customizable and low-cost strategy, which has already been used in previous studies to fabricate bioreactors for *in-vitro* cell culture [20], as well as AD [21]. 3D-printed components are reusable and have been considered as an excellent option for analyzing microbe-mediated bioenergy systems [21]. By coupling such a tailor-made, purpose-oriented bioreactor design to programmable data collection software, and equipped with multiple sensor ports, a high level of flexibility of such an experimental concept is achieved.

2. Material and methods

2.1. 3D-printed tailor-made PFR

The PFR module, as used in this study, consisted of a vessel, which was a horizontal cylinder made of clear extruded acrylic glass of a length of 750 mm, inner diameter of 144 mm, thickness of 3 mm, with a total volume of 12.2L. The dimensions and positions for sampling ports and sensors are shown in Fig. 1. STL-files about the 3D-print of the 3-blade stirrers, the inside/outside washers and seal plates at the sensor ports and dimensions of electrode holders are added as supplementary material.

The parts of the PFR module are briefly described in the following: Side plates are made of PTFE. They have a ring groove into which the reactor vessel is fitted. In between, an O-ring seals the connection, supported with transparent silicone rubber (Liqui Moly GmbH, Ulm, Germany). Both side plates are equipped with Iglidur X sleeve bearings (IGUS GmbH, Cologne, Germany) in the center to hold a stirrer shaft made of stainless steel (V4A) with a diameter of 15 mm and a length of 770 mm. The stirrer shaft is sealed with a shaft seal made of fluororubber (HUG Technik Shop GmbH, Ergolding, Germany) at the inner part of one side plate and is fixed by another side plate made of polyoxymethylene with a thickness of 15 mm. A polyoxymethylene side plate is also used at the side of the outlet to stabilize the construction and to avoid bending of the PTFE side plate. Five 3-blade stirrers are 3D-printed with PA2200 white Nylon (nano sealed plus slide finished), and clamped onto the stirrer shaft with stainless steel clamp rings (Mädler GmbH, Hamburg, Germany). The distances of stirrer blades from the end of the stirrer shaft are 90, 240, 420, 555 and 670 mm. An IKA Eurostar40 stirrer (IKA®-Werke GmbH & Co. KG, Staufen, Germany) is used as motor. Ports for feed and harvest are made of PVC grommets (ID = 20 mm, ¾" external thread) with clamping nuts. A PVC tube (length = 100 mm, outer diameter = 20 mm) is clamped into the grommets and closed with a rubber plug. All sealing threads of the PFR are reinforced with Teflon tape.

At the bottom of the vessel, Hamilton ARC sensors (Hamilton Bonaduz AG, Bonaduz, Switzerland) were installed to measure conductivity (ConduCell UPW), pH-value (EasyFerm PHI) and redox potential (EasyFerm ORP) at the inlet, center, and outlet zone in the liquid phase. All sensors were additionally recording the temperature. The ARC sensors were mounted in electrode holders made of PETP, equipped with a sealing inside the vessel, which is 3D-printed with Silicone G1H Shore 65A and adjusted to the curvature of the reactor vessel pipe of the reactor. The washer is printed with white resin FORM2 (formlabs GmbH, Berlin, Germany). All electrodes were equipped with VP8 data cables (Hamilton) which were connected to a power source (Voltcraft HPS 13015) and a Modbus USB-RS485 converter (Hamilton). Hose connectors (10 mm/12 mm) made of POM were fixed into drillings (10 mm) on the reactor vessel and sealed with silicone rubber to connect the sampling ports at the inlet, center, and outlet of the reactor. A silicone

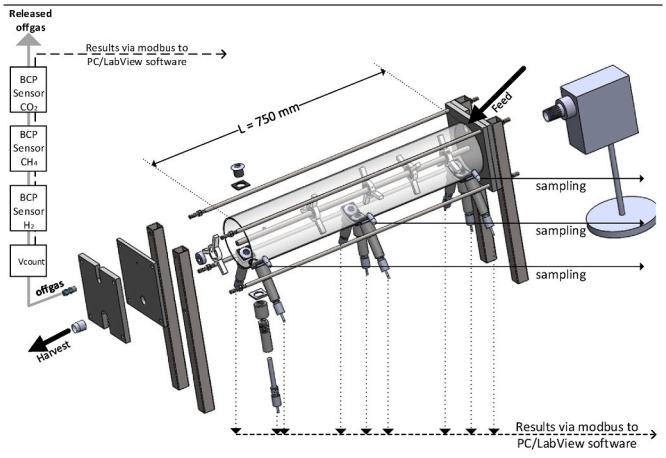

Fig. 1. Sketch drawing of the tailor-made plug-flow reactor made of a plexiglass tube and 3D-printed parts and operated with multi-position monitoring in the liquid phase.

hose (12 mm ID), which was closed with a hose clip, was connected to the hose nozzle for sampling. A polyethylene tubing (12 mm ID), which was connected to an Eco silver thermostat (Lauda GmbH, Lauda-Königshofen, Germany) was wrapped around the reactor vessel to improve temperature control. The reactor was additionally covered with insulating material made of latex foam with a thickness of 30 mm. A common QS push-in hose fitting was installed for the gas phase outlet connection at the top of the outlet side plate. The gas hoses were made of thermoplastic polyurethane. The off-gas volume was measured with a BlueVcount gas counter (BlueSens GmbH, Herten, Germany). Afterwards, the off-gas passed three BCP sensors (BlueSens) to determine the concentration of CO_2 (BCP–CO_2; max. range of 50 Vol-% CO_2), CH_4 (BCP–CH_4) and H_2 (BCP–H_2). The software BlueCheck (version 2.2.1.3, BlueSens) was used for data collection. All other data were recorded with LabView (version 2018 – National Instruments Corp. Ltd., Newbury, United Kingdom).

2.2. Process operation and sampling

The tailor-made PFR was used to perform anaerobic hydrolysis in a continuous DF mode, at 10 rpm, with agricultural residues, namely maize silage and grass silage as feedstock. Although not all of these feedstock components can be regarded as purely residual, they are suitable to serve as a model substrate. The starting inoculum was collected from a German industrial-scale biogas plant, which is continuously operated with MS (15% of DM) as main feedstock. Acidic pretreatment was performed as described elsewhere [3]. The reactor module was harvested and fed 5 times per week in order to meet the conditions as described in Table 1. Both, the fresh MS (87.9 ± 12.4% DM, 96.8 ± 0.02% VS) and bench-dried GS (93.1 ± 0.1% VS) were sieved with a mesh width of 5 mm. Samples of a volume of 15 mL were collected from ports at the inlet, center and outlet of the PFR twice a week, a portion was directly used for *at-line* measurements. The leftover was stored for a maximum of two weeks at −20 °C prior to *off-line* analysis. 16 mL of 85% (ww^{-1}) phosphoric acid was added to inactivate the methanogens.

2.3. At-line and off-line analysis

Several *at-line* and *off-line* measurements were conducted throughout the experiments.

2.3.1. At-line measurements of the frequency-dependent anisotropy polarizability (FDAP)

3 mL of the fresh samples were used for *at-line* measurements of the FDAP of cells (also known as cell polarizability as an estimate about the physiological state of a cell). Samples were prepared and analyzed as described by Gómez-Camacho et al. [3]. The FDAP was measured with EloTrace® (EloSystems GbR, Berlin, Germany) at frequencies of 200, 400, 900 and 2,100 kHz. The method follows the principles described by Bunin [22]. The displayed values of the FDAP do not contain the scale coefficient of $5{\cdot}10^{-31}$. Triplicate analyses were performed for each sample.

2.3.2. Off-line analysis

SCCAs. The SCCA composition in the liquid phase was determined using 2 mL of frozen samples, thawed at room temperature, and then stored at not more than 4 °C for 24 h for further salt precipitation. The samples were then centrifuged at 4 °C and 13,300×*g* for 20 min. The supernatant was filtered with a 0.2 μm Nylon filter (Carl Roth GmbH, Karlsruhe, Germany). Proteins were precipitated with a clarification kit (Carrez clarification, Merck KGaA, Darmstadt, Germany). A 1200-series HPLC system (Agilent Technologies Inc., Waldbronn, Germany), equipped with a refractive index detector and an HyperRez XP Carbohydrate H^+ column (Fisher Scientific Inc., Waltham, MA), was used for analysis as recently described by Camacho *et al.* [3].

Soluble chemical oxygen demand (sCOD). Thawed samples were filtered through a regenerated cellulose filter with a pore width of 0.45 μm (Merck) and diluted 100-fold in deionized water. 2 mL of liquid were transferred into a chemical oxygen demand mercury-free TNTplus vial test (Hach Lange GmbH, Düsseldorf, Germany), and analyzed according to the manufacturer's instructions.

FOS/TAC. 5 mL of sample volume were diluted in 50 mL of deionized water. The pH-value was adjusted to 8.5 (±0.2) with potassium hydroxide (25% wv^{-1}). Samples were analyzed by pH titration using the method described by Hach Lange®, adapted from the Nordmann's protocol, using a 0.05 M H_2SO_4 titrant solution under stirring [23,24].

Viscosity (η)**.** 40 mL of culture broth at room temperature were used for torque measurements in a power control-Visc P7 Viscoclick (IKA®). The torque measurements were used to calculate the viscosity [PaS] of the samples with equations (1) and (2) following the methodology as described in Ref. [25].

$$c(N_i) = 148.85N_i + 116.35 - \frac{9.188}{N_i} \tag{1}$$

$$\eta = \frac{2\pi \cdot N_m}{N_i \cdot D_i^3 \cdot c} \tag{2}$$

c is a constant factor, which was obtained by reference measurements within a pure glycerol solution and defined dilutions (1:1; 1:2; 1:3) of it, N_i is the stirring speed [s^{-1}], D_i is the vessel diameter [m], and N_m is the torque [Nm], which is measured at the stirrer shaft.

Reynolds number (Re). The Reynolds number for plug-flow was determined with equation (3) as described e.g. by Chen [26]:

$$Re = \frac{\boldsymbol{v}_m \cdot d}{\boldsymbol{\nu}} \tag{3}$$

Power input (P/V). The power input into the liquid phase of the reactor was calculated as described by Barradas *et al.* [27] with equation (4):

$$P = M \cdot \omega \tag{4}$$

2.4. Statistical analysis

Principal component analysis (PCA) was conducted with Origin (Pro) (version 16.1, OriginLab Corp., Northampton, MA) in order to identify correlations between *on-line* and *off-line* parameters. In case of the FDAP measurement, two PC score values were used as they contained a major linear independent information of the spectra. For regression analysis, the weekly average values of *on-line* measurements were used for comparison with *off-line* measurements, which were conducted less frequently. Values were normalized to their maximum values and analyzed via Pearson's correlation with SigmaPlot® (version 12.5, Systat Software Inc., San Jose, CA).

Table 1
Operational parameters of the plug-flow reactor.

Week [W]	Feedstock mixture	HRT [d]	OLR [g_{DM} L^{-1} d^{-1}]	Total DM [%]
0–6	MS	27.5 ± 4.3	1.5 ± 0.5	28 ± 1.5
7–10	1:1 MS:GS (DM)	16.4 ± 4.2	1.5 ± 0.5	24 ± 1.7

3. Results & discussion

The aim of this work was to investigate the usefulness of gradient measurements in the liquid phase of a digestion process in a continuously operated PFR. Therefore, not a steady but dynamic state with

changing process modes and cultivation conditions were applied to gain a variety of different parameter values. The chosen process modes were either full AD under increasingly acidic conditions (so-called acidification) or finally DF with a dominant hydrolytic and acidogenic phase under prevention of methanogenesis. Sensors for the measurement of the pH-value, the ORP and the conductivity were mounted into the liquid phase of the inlet, center and outlet part of a PFR. In the liquid phase, no foam formation was observed at all throughout the experiments. The *on-line* data were used for a linear regression analysis together with data from *at-line* and *off-line* measurements. Linear regression served as a basic method for the identification of obvious correlations. The *at-line* and *off-line* measurements included the concentration of side metabolites and measures of the cell physiology status. Along with the identification of correlations, the question was answered, whether a multi-position measurement and finally the determination of gradients can provide additional information about the process performance, and thus brings benefits in comparison to the common single-spot measurement at a usually arbitrarily chosen location along a PFR.

3.1. Flow characteristics and power input

To describe the systems' fluid flow behavior, the viscosity of the culture broth was measured and the Reynolds number for tubular flow was determined (Table 2). Typically, the Reynolds numbers, as obtained in this study, describe a strongly laminar plug-flow behavior, which is a requirement for the development of gradients along the reactor length. Possible back-mixing effects would counteract the development of gradients; however, the viscosity is several orders of magnitude higher than that of water, and therefore the inner friction within the fluid phase and between the fluid phase and vessel walls should theoretically prevent back mixing. The viscosity as determined in samples of this study is in the same order of magnitude as the one determined at 20 °C from activated sludge samples with a total solid content of 6% [28]. The actual development of gradients, as shown further in the results section, supports the assumption of a dominant plug-flow behavior.

3.2. Assessment of gradient formation in the plug-flow reactor

The digestion of agricultural residues in the PFR was examined with the following tools and methods: i) multi-position monitoring of the pH-value, ORP and conductivity at three different HRT in the PFR, ii) *on-line* monitoring of the CO_2, H_2 and CH_4 content in the gas phase at the outlet of the reactor and iii) corresponding *off-line* measurements of sCOD, FOS/TAC ratio, and SCCA concentrations in the liquid phase. The one-spot monitoring of the gas phase at the outlet of the reactor is assumed to be representative for the whole headspace under the assumption of a gradient-free gas phase as typically assumed in other studies [10].

Biogas is typically composed of 50% (v/v) or more CH_4 in full digestion, while the rest of the off-gas comprises of CO_2, 0–1% H_2, and 0–15% of N_2, H_2S, and probably traces of O_2 [29]. The gas composition during W0 – W6 leads to the assumption that the feeding of pure MS causes a higher release of CO_2 and H_2 in comparison to the subsequent feeding phase, during which a higher portion of the gas phase is likely composed of N_2. A final transition to a pure DF mode and the nearly total depletion of activities of methanogens is characterized by a CH_4 concentration drop from 18.9 ± 0.01% to 2.3 ± 0.15%, together with an increase of H_2 production from 1.54 ± 0.2% to 6.26 ± 1.5% (Fig. 2a) in the first three weeks. Hence, different conditions were achieved in the respective period: i) a process mode with a low activity of methanogenic organisms under acidification, and ii) a process mode with hardly any methanogenic activity, representing a DF. Both modes are dynamically changing throughout the time of observation in order to get a variety of data for the regression analysis and subsequent evaluation of the monitoring concept.

Table 2
Viscosity, Reynolds number and power input during operation of the plug-flow reactor.

Time [w]	Dynamic viscosity [Pa s]	*Reynolds* number	Power input [W m^{-3}]
0	3.9 ± 0.6	$2.5{\cdot}10^{-6}$	0.10
2	5.4 ± 0.9	$1.9{\cdot}10^{-6}$	0.11
4	4.9 ± 0.3	$2.4{\cdot}10^{-6}$	0.12
6	5.1 ± 0.6	$2.5{\cdot}10^{-6}$	0.18

The low pH-value at the outlet in the first phase is most likely due to a previously applied artificial acidification (addition of phosphoric acid through the outlet port). It hindered the action of microorganisms in the latter part of the reactor, thus the re-assimilation of side products like SCCAs might also have been affected negatively by a sudden drop of the pH-value below 5.0 [30,31]. Since methanogens are highly sensitive to low pH-values below 5.5 [32], the methanogenic stage was clearly suppressed and the level of CH_4 was very low from W2 on. Conditions were obviously dynamically changing in some areas of the PFR, while the measurement of the pH-value in the center part remained comparably stable. It is noteworthy to mention that most often, one-spot measurements in PFRs are conducted in the center part. It becomes obvious from Fig. 2 that many of the process dynamics cannot be caught at this zone.

The question remains, however, how relevant the changes, especially of the pH-value at the outlet zone, are for process monitoring and control. When considering the development of the conductivity values, it becomes obvious that most of the dynamic behavior was monitored at the second part of MS feeding, when the pH-value remained rather stable at all three positions across the reactor. In contrast, the conductivity showed a very dynamic behavior from the inlet through the center to the outlet position during the whole observation period. Values from the inlet and center part reflect obviously best the synthesis of SCCAs. Dynamic changes were also recorded by the ORP over the whole period. In waste activated sludge alkali pre-treatment tests, the sCOD content was predicted from ORP values, as a positive correlation existed between these parameters. This strong correlation (R = 0.96) shows that the ORP-values can be used to predict the solubilization efficiency of the waste activated sludge [15]. In the present study, however, sCOD values show an increasing trend with the experimental time, with a slight decrease in parallel to the HRT (Fig. 3c). There is no clear correlation visible at a first sight, however, the sCOD increased from W0–W6 and decreased with the substrate changes from W7 on (Fig. 3c) together with the accumulation of total SCCAs (Fig. 3a).

In general, results of the first weeks are in accordance to expectations: a low pH-value in hydrolysis and acidogenesis leads to an increase of the H_2 production as shown in a double-stage AD of MS for both, the H_2 and CH_4 production [33] and for many biogenic feedstock and for agricultural waste [34]. The low off-gas concentration of CO_2 and H_2 after the change from MS to MS/GS co-feeding is probably due to an overall lower bacterial growth as before, as an accumulation of butyric acid up to 8.5 ± 0.4 g L^{-1} at the outlet might have hindered biomass formation (Fig. 3b). A similar trend was already seen in the first part of pure MS feeding (Fig. 3a). Indeed, in the present study, the acidogenic phase is dominated by butyric acid, while the accumulation of acetic acid was relatively low (0.6 ± 0.1 to 1.5 ± 0.08 g L^{-1}, **data not shown**). The production of butyric acid induces self-inhibition [35], which limits biomass growth and H_2 production. Thus, N_2 remains the dominant part of the gas phase.

SCCA concentrations were rather similarly distributed along the reactor. Biggest concentration gradients were seen at the outlet part. As also previously described for similar conditions of biogenic waste AD for biogas production, with an HRT of 16d and an OLR of 14 $g_{VS}L^{-1}d^{-1}$, the SCCAs concentration tends to decrease along the reactor length [36]. This shows that most of the acid accumulation happened in the first part of the reactor, while subsequently, either production and re-assimilation were rather equal or synthesis ceased. A lower SCCA concentration at

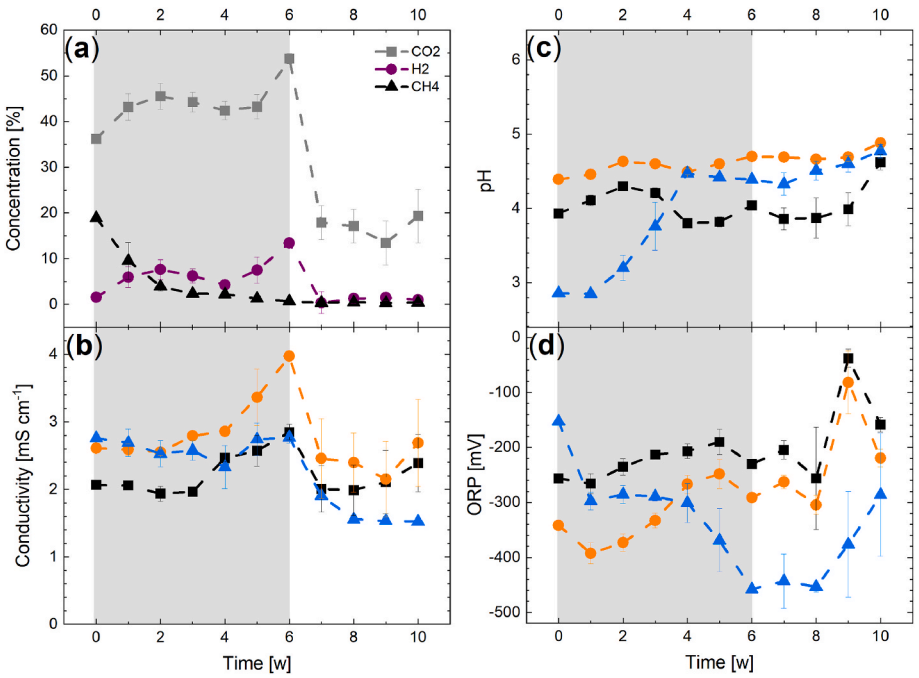

Fig. 2. *On-line* monitoring during acidified digestion of agricultural feedstock in a plug-flow reactor. *On-line* measurements of the gas phase (**a**) and measurements for the multi-position *on-line* monitoring of the conductivity (**b**), pH (**c**) and ORP (**d**) in the liquid phase at the inlet, center, and outlet part of the PFR are depicted by black squares, orange circles, and blue triangles, respectively. The period of feeding MS is depicted in grey (W0 – W6), while the period of feeding with MS:GS feedstock mix is depicted in white (W7 – W10). In both periods, an OLR of 1.5 ± 0.5 g_{DM} L^{-1} d^{-1} was applied. (For interpretation of the references to colour in this figure legend, the reader is referred to the Web version of this article.)

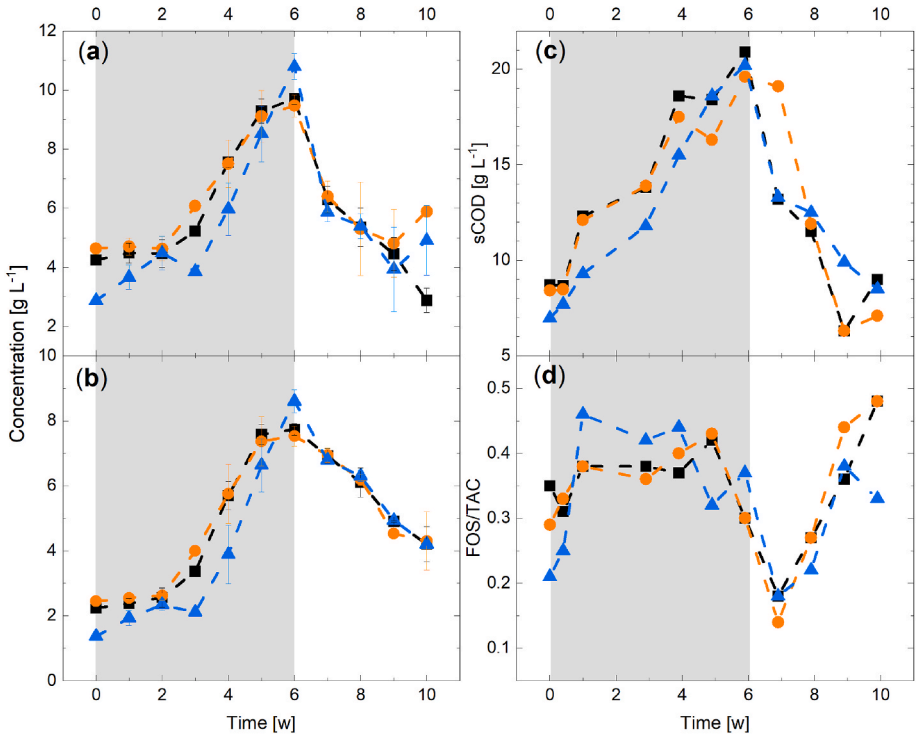

Fig. 3. *Off-line* parameters during acidified digestion of agricultural feedstock in a plug-flow reactor. Samples of the liquid phase from the inlet (black squares), center (orange circles), and outlet (blue triangles) of the PFR were analyzed for the total SCCA (**a**) and butyric acid (**b**) concentrations, sCOD (**c**) and FOS/TAC (**d**). MS (grey area) and a GS:MS mix (white area) were used as feedstock with a final OLR of 1.5 ± 0.5 g_{DM} L^{-1} d^{-1}. (For interpretation of the references to colour in this figure legend, the reader is referred to the Web version of this article.)

the outlet up to W5 suggests their re-assimilation between the center and outlet part. While spatial gradients were small, the synthesis itself was highly dynamic under the different process conditions. The accumulation of SCCAs started to increase subsequently from W3 on. Most likely, an adaptation and/or stabilization of the microbiota after the previous artificial acidification led to this increase [37]. Not surprisingly, the highest accumulation of SCCAs, namely 10.8 ± 0.4 g L^{-1} at the outlet, appears in parallel with the highest H_2 concentration in the off-gas (13.5 ± 0.7 Vol-%) in W6, but not to the lowest pH-value, which occurred before. The decrease of H_2 and CO_2 concentrations (Fig. 2a) at the strongest increase of butyric and acetic acid concentrations (Fig. 3b) before W6 might be explained by the presence of strictly anaerobic acetogens using the Wood-Ljungdahl pathway. They consume CO_2 and H_2 for acetyl-CoA synthesis, and subsequently acetic and butyric acid production. Among these microorganisms are typically *Eubacterium* spp., *Butyribacterium* spp. and *Clostridium* spp. [38]. This is also reflected in the ORP profile (Fig. 2d), where low values (below −240 mV) describe a state with a low concentration of H^+, which is converted to H_2O through the Wood-Ljungdahl pathway, while an increase might be due to a higher H^+ concentration and the presence of reducing agents

from W8 on. A low ORP value can be a sign for a an accelerated butyric acid production [39].

The determination of FOS/TAC values are a suitable and frequently applied analysis to control feeding of a continuous process. A value between 0.4 and 0.6 is considered optimal. Below 0.4, the system is considered to be operated at starvation, above 0.6 it is usually considered to be overfed [40]. Hence, starvation conditions were detectable throughout certain weeks of operation. The gradient observed in the FOS/TAC ratio at W0 suggests a non-linear distribution and consumption of the feedstock, reflecting the process of microbial segregation and adaptation in dependence of the HRT. The gradient was lower at short HRTs (0.35 ± 0.3 d at the inlet and 0.33 ± 0.3 d at the center during the first 3 weeks of operation). The COD and sCOD are values that characterize indirectly the amount of material that can be degraded in the liquid phase [41,42]. High values indicate either a high load of fresh feedstock or a slow degradation process as it was detectable in the middle of the experiment. This is exactly where the metabolic activity decreased, which might have caused this dynamic behavior (Fig. 3c and d).

3.3. At-line monitoring of frequency-dispersed anisotropy polarizability

The polarizability of a cell suspension depends on the cell's physiological state, while the time of response to an electrical field intensity change depends on the electron content and conductivity in cell components. The electrooptically determined polarizability has been used as a predictive method for the cells' activity to metabolize substrates and release products, also in anaerobic cultivation. FDAP was used for metabolic flux prediction and the estimation of the cell shape and length, as e.g. applied for *Clostridium acetobutylicum* batch cultures [43]. This measurement technology was included in our study to gain additional information that could be correlated with the *on-line* measurements in the liquid phase. Since both, the FOS/TAC and sCOD, as well as the accumulation of SCCAs, showed a highly dynamic behavior, the physiological cell status should also have changed during the course of the experiment.

In our study, no major differences were observed for the measurements at higher frequencies of 900 and 2,100 kHz, while variations were observed for measurements at 200 and 400 kHz at the inlet, center and outlet of the PFR (Fig. 4, S1). Acidification conditions, as applied here, put cells under environmental stress. The transport mechanisms through the cell wall are likely affected, possibly because the acid flow is redirected to uptake and conversion into other products. A gradient formation along the HRT was detected, in which cell viability and activity are the lowest at the outlet of the reactor, where the pH-values are also the lowest (between W0 and W2) and methanogens are distressed by growth conditions. In between W3 and W5, cell viability and activity are higher during hydrolysis and acidogenesis at shorter HRTs, as a response to the acidification strategy in the PFR, reflecting microbial adaptation and process stabilization. This is in good agreement with the increase of the SCCAs production (W3, Fig. 3a), while the pH-value remains stable during this phase (W4, Fig. 2c). Studies with *E. coli* (and other microorganisms) showed that variations in the FDAP allow to distinguish between high and low consumption of substrates [44], also in DF [3]. The signal intensity's increase in samples of week 1 and 5 reflects the microbial adaptation to the acidified process mode (and finally DF) in parallel with accelerated synthesis. The decrease in FDAP in weeks 3–6 at the inlet and center part of the reactor (Fig. 4a and b) could be a response to induced stress by the accumulation of SCCAs up to 9.7 ± 0.2 and 9.5 ± 0.4 g L^{-1}, respectively (Fig. 3a). Rather constant values of the FDAP at the outlet can be explained by a better adapted microbiota to acidogenic conditions, leading to an SCCA accumulation up to 10.8 ± 0.6 g L^{-1} (Fig. 3a). The further decrease from W7 on is mostly due to the low FOS/TAC ratio and a low sCOD value. In parallel to the low polarizability, the concentration of SCCAs declines. It is noteworthy that the values at the inlet are consistently higher because, as is evident from the higher FOS/TAC values, there is likely more substrate available. The deviations for some measurements, however, are large, so any interpretation has to be taken with care.

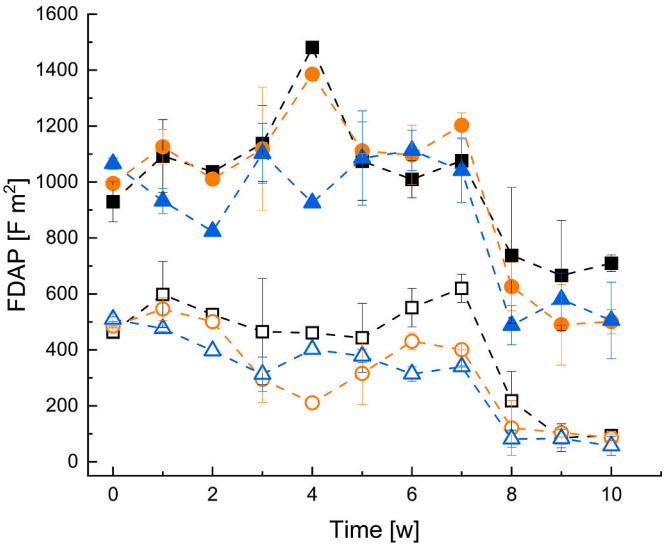

Fig. 4. Electrooptical measurement of the frequency-dispersed anisotropy polarizability (FDAP) as measured at frequencies of 200 kHz (empty dots) and 400 kHz (full dots) in cell suspension samples from the inlet (black squares), center (orange circles) and outlet (blue triangles) in acidified full digestion in a plug-flow bioreactor. (For interpretation of the references to colour in this figure legend, the reader is referred to the Web version of this article.)

Results show that the metabolic activity and cell physiology evolve along the reactor length from a high metabolic activity for hydrolysis and SCCAs production at the beginning and for the presence of considerably high amounts of SCCAs at the outlet of the PFR, reinforcing the conclusion that one-spot *on-line* monitoring might not be sufficient to catch the potentially different responses of cells, especially when comparing the state at the outlet to the other reactor zones.

3.4. Benefits of multi-position monitoring in plug-flow digestion

In order to assess eventual benefits of multi-position measurements for gradient monitoring in the PFR-based digestion, Pearson's correlations were determined for the average of weekly gained values of the *on-line*, *at-line* and *off-line* measurements during W0 and W6. The goal of this study was to examine if there are benefits of multiposition *on-line* monitoring at process disturbances and if at least some *off-line* analysis can be replaced or efforts be reduced. Therefore, correlations between *off-line* (PC1, PC2 and SCCAs) and *on-line* (pH, ORP, and conductivity) monitored parameters were analyzed. Not surprisingly, CO_2 and H_2 contents in the off-gas depict a strong positive correlation, both values correlate negatively to the CH_4 content. This is typical as the accumulation of both gases are a sign of low activity of methanogens [29]. Similarly, for the same reason, the CH_4 content also tends to be negatively correlated with the SCCAs concentration at all ports (Fig. 5a–c).

The pH-values depict positive correlations with PC1 (gained from the FDAP spectra, Fig. S1) at the inlet port of the PFR (Fig. 5a), however this correlation is not present at the center and outlet ports, possibly because the pH gradient disappeared at longer HRTs (center – outlet) around W4 when the process became rather completely acidified. Good correlations have also been found between ORP and SCCA production at center and outlet ports (Fig. 5b and c). However, while these correlations were positive at the center part, a negative correlation was found at the outlet of the PFR. This is possibly due to the fact that ORP values depict a decreasing trend at the outlet of the reactor (recall Fig. 2d), but the SCCA concentrations did not reflect such behavior (Fig. 3a and b). The ORP is known to correlate positively with the sCOD content, but it shows a

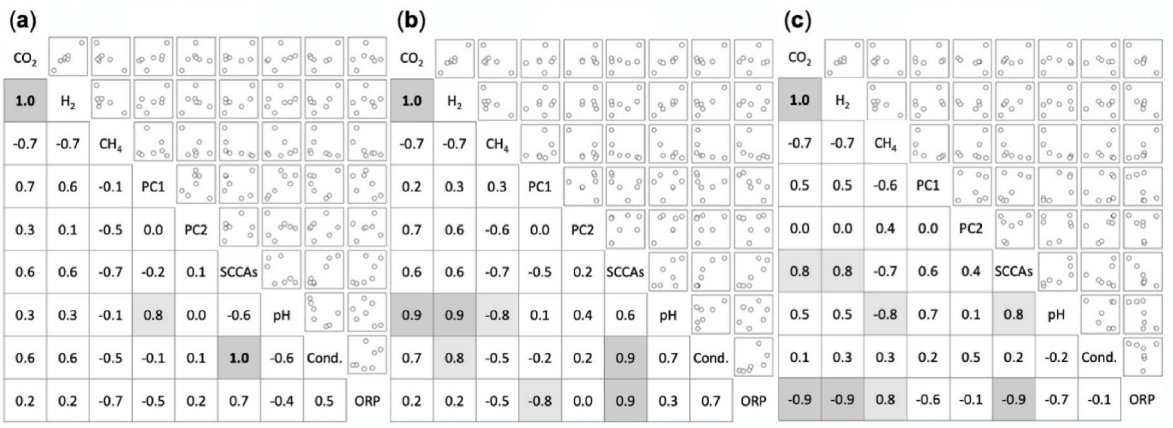

Fig. 5. Pearson's correlation coefficients for local measurements at the inlet (**a**) center (**b**) and outlet (**c**) in acidified digestion in a plug-flow bioreactor during weeks 1–6. The average of the local measurement values of pH, conductivity and ORP, CO_2, H_2 and CH_4 during a week and *at-line* measurements of the FDAP represented by PC scores 1&2 and *off-line* measurements of the SCCA accumulation at each port were considered.

negative correlation with the pH-value, as it has been also observed for the solubilization of waste activated sludge [15]. Indeed, a negative correlation trend has been observed at the outlet port between ORP and pH-values, suggesting that the pH-value affects the ORP more than the sCOD content in our study. Conductivity depicts a strong positive correlation with the SCCAs accumulation at the inlet and center ports, however, the correlation is lost for longer HRTs at the outlet of the reactor. Additionally, good correlations between the conductivity and pH-values, as well as CO_2 and H_2 content in the off-gas were observed at the center of the PFR. These observations are in good agreement with previous studies, which have suggested that conductivity can be used as a monitoring parameter for biogas production, pH-value and SCCA accumulation in AD processes [16,17].

Overall, the various correlations found between the *on-line* and the *off-line* parameters indicate that the application of sensors in different positions along a PFR for monitoring the gradients can be advantageous over monitoring at a single-position in a dark fermentation mode.

Among the most important *off-line* parameters that describe the process disturbance under unwanted acidification or the process performance in DF mode is the accumulation of SCCAs. At the inlet, the SCCA accumulation positively correlated with the conductivity measurements (Fig. 5a). At the center part, SCCA accumulation positively correlated with the conductivity and ORP measurements (Fig. 5b). However, at the outlet (Fig. 5c), the SCCA accumulation negatively correlated with the ORP measurements and positively with pH-vales. This may indicate that measuring the pH at different locations does not provide additional information, but that, different of what is done in practice, the outlet is a better location for a pH probe than the center. It is interesting though that measurements are correlated positively, which also provides a hint that a drop in the pH-value at the outlet part of the PFR might prevent a further accumulation of SCCAs (too strong acidification and loss in process performance). In contrast, if only low SCCA concentrations would appear (below the values obtained throughout our experiments), the pH-value would naturally remain higher. Then, the relation as described previously between the SCCAs concentration and the pH-value would not make sense. Hence, the identified correlation might only be valid below a certain threshold pH-value. Additionally, as it can be seen at the SCCA accumulation against conductivity plots at the inlet and center (Fig. 5a and b) as well as against the pH-values at the outlet (Fig. 5c), the curve is following a non-linear behavior. Thus, applying non-linear correlation yields greater determination coefficients.

To investigate possible further advantages of the *on-line* measurements to detect process disturbances, the acquisition of spatial gradients rather than local measurements was investigated by performing a linear correlation analysis with respect to gradients between the inlet and center (IC), as well as the center and outlet (CO) part. It is shown in Fig. 6 that the IC and CO gradients develop differently in the liquid phase and consequently show different correlations. Naturally, the correlations found for the off-gas contents regarding CO_2, H_2, and CH_4 are consistent with what has been observed in local measurements. No strong correlation was found between the gradient of SCCA concentrations and the *on-line* monitored parameter gradients of the pH-value, conductivity and ORP, neither for the IC nor the CO part (Fig. 6). Moreover, the CO_2 and H_2 concentrations correlate positively with the SCCA concentration gradient in the CO part and, interestingly, the pH gradient correlates also positively with the gradient of the PC1 from the FDAP spectra in the CO part (Fig. 6b). This means that an increased gradient of the pH-value favors a higher FDAP value in the outlet part of the bioreactor. No other correlations between the gradients of *on-line* and *off-line* monitored parameters have been found in this study. The pH-values, however, depict a negative correlation with other *on-line* monitored parameters, namely the conductivity and ORP for the CO (Fig. 6b), as well as a positive correlation with ORP for the IC (Fig. 6a). The latter also presents a positive correlation with the conductivity in the CO part (Fig. 6b).

Concerning the gas production, the strong positive correlation of the CO_2 and H_2 content with conductivity at shorter HRTs, but strong negative correlation with both conductivity and ORP at longer HRTs, suggests that production has been favored only at the inlet and center of the reactor, during hydrolysis and acidogenesis. In fact, methane was only produced at the expense of these gases at longer HRTs, as shown by the positive correlation between the CH_4 content, conductivity and ORP in the CO part (Fig. 6b).

4. Conclusion and outlook

Acidification and DF represent either a process disturbance of a full digestion or an interesting process mode if SCCAs and H_2 shall be the final products. In our study, it was investigated if multi-position monitoring in the liquid phase can contribute to detect acidification early or maintain a DF state better than with a common one-spot measurement in a plug-flow bioreactor. Overall, the local measurements are beneficial at the inlet and center ports for the conductivity measurements, at the center and outlet ports for the ORP measurements and at the outlet port for the pH measurement with respect to the SCCA accumulation. This SCCA accumulation is one of the most interesting parameters to be predicted by *on-line* measurements. In case of the spatial gradient acquisition, the conductivity gradients in the first and second part of the plug-flow bioreactor are correlated with CO_2 and H_2 accumulation. Gradients of the ORP in the center to outlet part of the bioreactor

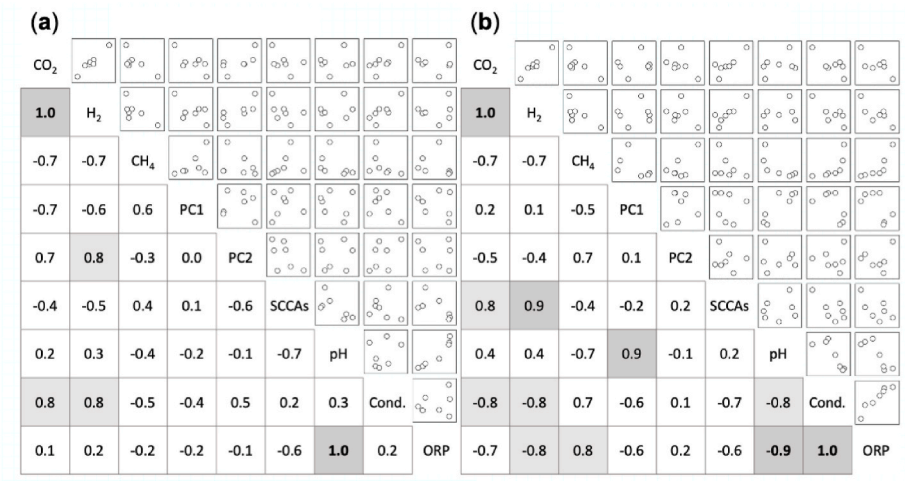

Fig. 6. Pearson's correlation coefficients for gradient formation between the inlet and center (**a**) as well as in between center and outlet (**b**) in acidified digestion in a plug-flow bioreactor. The average of the local measurement values of pH, conductivity and oxidoreduction potential, CO_2, H_2 and CH_4 during a week and *at-line* measurements of the FDAP represented by PC scores 1&2 and *off-line* measurements of the SCCA accumulation at each port were considered; gradient scores were calculated between the inlet to center and center to outlet prior to the correlation analysis.

correlate with H_2 accumulation in the off-gas. However, no clear benefits from the measurement of gradient formation with respect to the SCCA accumulation were observable. Interestingly, the pH gradient in the inlet to center part correlates with the first PC of the cell polarizability spectrum. Further process states and disturbances will be applied in future studies to prove whether the correlations that were found are consistent over a wide range of operation modes or if other or further benefits will occur at those cases.

Together with an expert system built based on the gradient acquisition of selected local measurements of conductivity, ORP and the pH-value, improved process monitoring and control can be achieved. This finding is relevant as independent, well-controllable operation is particularly required in decentralized production concepts. These allow an operation close to the source of biogenic feedstock, ideally residues, when transport is too costly or hardly feasible, like in remote regions in many countries of the world. The demonstrated concept in a low-cost tailor-made lab reactor with installation costs of approx. 1,500 € (w/o the sensor technology) allows to examine many feedstock combinations and monitoring strategies in plug-flow digestion processes. Any progress to increase the autonomous operation of such processes would contribute to an increased amount of material that can be valorized either for energy or material use.

Statements & declarations

The authors declare to have no conflicts of interest.

Data availability

Data of this article is available from the authors upon a reasonable request.

Acknowledgments and Fundings

This work was part of the European joint research project „PASS-BIO - Plug-flow reactor-based Acid fermentation for Small-Scale BIO-refineries", and as such funded by the German Federal Ministry of Education and Research in the frame of the ERA-NET cofund FACCE-SURPLUS, grant no. 031B0659.

Abbreviations

AD	anaerobic digestion
CO	center to outlet
COD	chemical oxygen demand
CSTRs	continuous stirred tank reactors
DF	dark fermentation
DHA	docosahexaenoic acid
DM	dry matter
EPA	eicosapentaenoic acid
GS	grass silage
HRT	hydraulic retention time
IC	inlet to center
ID	inner diameter
MS	maize silage
ORP	oxidoreduction potential
PC	principal component
PETP	polyethylene terephthalate
PFR	plug-flow reactor
PFTE	polytetrafluoroethylene
PHAs	polyhydroxyalkanoates
PVC	polyvinyl chloride
SCCAs	short-chain carboxylic acids
sCOD	soluble chemical oxygen demand
TOC	total organic carbon
TS	total solids
VS	volatile solids

Appendix A. Supplementary data

Supplementary data to this article can be found online at https://doi.org/10.1016/j.biombioe.2023.106803.

References

[1] T. Menzel, P. Neubauer, S. Junne, Role of microbial hydrolysis in anaerobic digestion, Energies 13 (2020), https://doi.org/10.3390/en13215555.
[2] S.A.A. Rawoof, P.S. Kumar, D.V.N. Vo, S. Subramanian, Sequential production of hydrogen and methane by anaerobic digestion of organic wastes: a review, Environ. Chem. Lett. (2020), https://doi.org/10.1007/s10311-020-01122-6.
[3] C.E. Gómez-Camacho, K. Pellicer Alborch, A. Bockisch, P. Neubauer, S. Junne, B. Ruggeri, Monitoring the physiological state in the dark fermentation of maize/grass silage using flow cytometry and electrooptic polarizability measurements, Bioenergy Res (2020), https://doi.org/10.1007/s12155-020-10184-x.
[4] S. Dahiya, O. Sarkar, Y.V. Swamy, S. Venkata Mohan, Acidogenic fermentation of food waste for volatile fatty acid production with co-generation of biohydrogen, Bioresour. Technol. 182 (2015) 103–113, https://doi.org/10.1016/j.biortech.2015.01.007.
[5] O. Sarkar, R. Katakojwala, S. Venkata Mohan, Low carbon hydrogen production from a waste-based biorefinery system and environmental sustainability assessment, Green Chem. 23 (2021) 561–574, https://doi.org/10.1039/d0gc03063e.
[6] G. Strazzera, F. Battista, N.H. Garcia, N. Frison, D. Bolzonella, Volatile fatty acids production from food wastes for biorefinery platforms: a review, J. Environ. Manag. 226 (2018) 278–288, https://doi.org/10.1016/j.jenvman.2018.08.039.
[7] A. Patel, O. Sarkar, U. Rova, P. Christakopoulos, L. Matsakas, Valorization of volatile fatty acids derived from low-cost organic waste for lipogenesis in

oleaginous microorganisms-A review, Bioresour. Technol. 321 (2021), 124457, https://doi.org/10.1016/j.biortech.2020.124457.
[8] M.F.M.A. Zamri, S. Hasmady, A. Akhiar, F. Ideris, A.H. Shamsuddin, M. Mofijur, I. M.R. Fattah, T.M.I. Mahlia, A comprehensive review on anaerobic digestion of organic fraction of municipal solid waste, Renew. Sustain. Energy Rev. 137 (2021), 110637, https://doi.org/10.1016/j.rser.2020.110637.
[9] R. Nkuna, A. Roopnarain, C. Rashama, R. Adeleke, Insights into organic loading rates of anaerobic digestion for biogas production: a review, Crit. Rev. Biotechnol. 42 (2022) 487–507, https://doi.org/10.1080/07388551.2021.1942778.
[10] P. Namsree, W. Suvajittanont, C. Puttanlek, D. Uttapap, V. Rungsardthong, Anaerobic digestion of pineapple pulp and peel in a plug-flow reactor, J. Environ. Manag. 110 (2012) 40–47, https://doi.org/10.1016/j.jenvman.2012.05.017.
[11] H. Escalante-Hernández, L.D.P. Castro-Molano, V. Besson, J. Jaimes-Estévez, Feasibility of the anaerobic digestion of cheese whey in a Plug Flow Reactor (PFR) under local conditions, Ing. Invest. Tecnol. 18 (2017) 264–277, https://doi.org/10.22201/fi.25940732e.2017.18n3.024.
[12] D.E. Arias, C. Veluchamy, M.B. Habash, B.H. Gilroyed, Biogas production, waste stabilization efficiency, and hygienization potential of a mesophilic anaerobic plug flow reactor processing swine manure and corn stover, J. Environ. Manag. 284 (2021), 112027, https://doi.org/10.1016/j.jenvman.2021.112027.
[13] D. Wu, L. Li, X. Zhao, Y. Peng, P. Yang, X. Peng, Anaerobic digestion: a review on process monitoring, Renew. Sustain. Energy Rev. 103 (2019) 1–12, https://doi.org/10.1016/j.rser.2018.12.039.
[14] A. Bockisch, E. Kielhorn, P. Neubauer, S. Junne, Process analytical technologies to monitor the liquid phase of anaerobic cultures, Process Biochem. 76 (2019) 1–10, https://doi.org/10.1016/j.procbio.2018.10.005.
[15] C.N. Chang, Y.S. Ma, C.W. Lo, Application of oxidation-reduction potential as a controlling parameter in waste activated sludge hydrolysis, Chem. Eng. J. 90 (2002) 273–281, https://doi.org/10.1016/S1385-8947(02)00015-3.
[16] C.A. Aceves-Lara, E. Latrille, T. Conte, J.P. Steyer, Online estimation of VFA, alkalinity and bicarbonate concentrations by electrical conductivity measurement during anaerobic fermentation, Water Sci. Technol. 65 (2012) 1281–1289, https://doi.org/10.2166/wst.2012.703.
[17] O. Marín-Peña, A. Alvarado-Lassman, N.A. Vallejo-Cantú, I. Juárez-Barojas, J. P. Rodríguez-Jarquín, A. Martínez-Sibaja, Electrical conductivity for monitoring the expansion of the support material in an anaerobic biofilm reactor, Processes 8 (2020), https://doi.org/10.3390/pr8010077.
[18] A. Robles, E. Latrille, J. Ribes, N. Bernet, J.P. Steyer, Electrical conductivity as a state indicator for the start-up period of anaerobic fixed-bed reactors, Water Sci. Technol. 73 (2016) 2294–2300, https://doi.org/10.2166/wst.2016.031.
[19] L. Moeller, A. Zehnsdorf, Process upsets in a full-scale anaerobic digestion bioreactor: over-acidification and foam formation during biogas production, Energy. Sustain. Soc. 6 (2016), https://doi.org/10.1186/s13705-016-0095-7.
[20] A.R. Raveling, S.K. Theodossiou, N.R. Schiele, A 3D printed mechanical bioreactor for investigating mechanobiology and soft tissue mechanics, MethodsX 5 (2018) 924–932, https://doi.org/10.1016/j.mex.2018.08.001.
[21] S. Achinas, G. Euverink, Development of an anaerobic digestion screening system using 3D-printed mini-bioreactors, IntechOpen, in: New Adv. Ferment. Process., 2019, https://doi.org/10.5772/intechopen.88623.
[22] V.D. Bunin, Electrooptical analysis of a suspension of cells and its structures, in: A. T. Hubbard (Ed.), Encycl. Surf. Colloid Sci., first ed., Marcel Dekker, New York, 2002, pp. 2032–2043.
[23] M. Lili, G. Biró, E. Sulyok, M. Petis, J. Borbély, J. Tamás, Novel approach on the basis of FOS/TAC method, Proceedings of the Analele Universităţii din Oradea, Fascicula Protectia Mediului, Oradea (2011) 713–718. http://protmed.uoradea.ro/facultate/anale/protectia_mediului/2011B/im/15.%20Mezes%20Lili.pdf.
[24] HACH company, Determination of FOS/TAC value in biogas reactors, 0–1, https://doi.org/10.1037/0022-3514.67.3.485, 2014.
[25] U. Schimpf, A. Hanreich, P. Mähnert, T. Unmack, S. Junne, J. Renpenning, R. Lopez-Ulibarri, Improving the efficiency of large-scale biogas processes: pectinolytic enzymes accelerate the lignocellulose degradation, J. Sustain. Energy Environ. 4 (2013) 53–60. https://www.thaiscience.info/journals/Article/JOSE/10889731.pdf.
[26] Y.R. Chen, Impeller power consumption in mixing livestock manure slurries, Trans. ASAE (Am. Soc. Agric. Eng.) 24 (1981) 187–192, https://doi.org/10.13031/2013.34222.
[27] O. Platas Barradas, U. Jandt, L. Da Minh Phan, M. Villanueva, A. Rath, U. Reichl, E. Schräder, S. Scholz, T. Noll, V. Sandig, R. Pörtner, A.-P. Zeng, Criteria for bioreactor comparison and operation standardisation during process development for mammalian cell culture, BMC Proc. 5 (2011) P47, https://doi.org/10.1186/1753-6561-5-s8-p47.
[28] P. Wei, Q. Tan, W. Uijttewaal, J.B. van Lier, M. de Kreuk, Experimental and mathematical characterisation of the rheological instability of concentrated waste activated sludge subject to anaerobic digestion, Chem. Eng. J. 349 (2018) 318–326, https://doi.org/10.1016/j.cej.2018.04.108.
[29] A. Anukam, A. Mohammadi, M. Naqvi, K. Granström, A review of the chemistry of anaerobic digestion: methods of accelerating and optimizing process efficiency, Processes 7 (2019) 504, https://doi.org/10.3390/pr7080504.
[30] Y. Lu, Q. Zhang, X. Wang, X. Zhou, J. Zhu, Effect of pH on volatile fatty acid production from anaerobic digestion of potato peel waste, Bioresour. Technol. 316 (2020) 3–10, https://doi.org/10.1016/j.biortech.2020.123851.
[31] Y. Li, D. Hua, J. Zhang, Y. Zhao, H. Xu, X. Liang, X. Zhang, Volatile fatty acids distribution during acidogenesis of algal residues with pH control, World J. Microbiol. Biotechnol. 29 (2013) 1067–1073, https://doi.org/10.1007/s11274-013-1270-z.
[32] M.A. Latif, C.M. Mehta, D.J. Batstone, Influence of low pH on continuous anaerobic digestion of waste activated sludge, Water Res. 113 (2017) 42–49, https://doi.org/10.1016/j.watres.2017.02.002.
[33] P.C. Benito Martin, M. Schlienz, M. Greger, Production of bio-hydrogen and methane during semi-continuous digestion of maize silage in a two-stage system, Int. J. Hydrogen Energy 42 (2017) 5768–5779, https://doi.org/10.1016/j.ijhydene.2017.01.020.
[34] J. Lindner, S. Zielonka, H. Oechsner, A. Lemmer, Is the continuous two-stage anaerobic digestion process well suited for all substrates? Bioresour. Technol. 200 (2016) 470–476, https://doi.org/10.1016/j.biortech.2015.10.052.
[35] A.K. Jha, J. Li, Y. Yuan, N. Baral, B. Ai, A review on bio-butyric acid production and its optimization, Int. J. Agric. Biol. 16 (2014) 1019–1024.
[36] E. Rossi, S. Becarelli, I. Pecorini, S. Di Gregorio, R. Iannelli, Anaerobic digestion of the organic fraction of municipal solid waste in plug-flow reactors: focus on bacterial community metabolic pathways, Water (Switzerland) (2022) 14, https://doi.org/10.3390/w14020195.
[37] J. Garcia-Aguirre, E. Aymerich, J. González-Mtnez, de Goñi, M. Esteban-Gutiérrez, Selective VFA production potential from organic waste streams: assessing temperature and pH influence, Bioresour. Technol. 244 (2017) 1081–1088, https://doi.org/10.1016/j.biortech.2017.07.187.
[38] H.L. Drake, Acetogenesis, in: Chapman, Hall (Eds.), Acetogenesis, Springer Science & Business Media, New York, 1994, pp. 3–60.
[39] K. Schuchmann, V. Müller, Energetics and application of heterotrophy in acetogenic bacteria, Appl. Environ. Microbiol. 82 (2016) 4056–4069, https://doi.org/10.1128/AEM.00882-16.
[40] R. Nkuna, A. Roopnarain, C. Rashama, R. Adeleke, Insights into organic loading rates of anaerobic digestion for biogas production: a review, Crit. Rev. Biotechnol. 42 (2022) 487–507, https://doi.org/10.1080/07388551.2021.1942778.
[41] A. Donoso-Bravo, C. Sadino-Riquelme, D. Gómez, C. Segura, E. Valdebenito, F. Hansen, Modelling of an anaerobic plug-flow reactor. Process analysis and evaluation approaches with non-ideal mixing considerations, Bioresour. Technol. 260 (2018) 95–104, https://doi.org/10.1016/j.biortech.2018.03.082.
[42] M. Arnell, S. Astals, L. Åmand, D.J. Batstone, P.D. Jensen, U. Jeppsson, Modelling anaerobic co-digestion in Benchmark Simulation Model No. 2: parameter estimation, substrate characterisation and plant-wide integration, Water Res. 98 (2016) 138–146, https://doi.org/10.1016/j.watres.2016.03.070.
[43] S. Junne, E. Klein, A. Angersbach, P. Goetz, Electrooptical measurements for monitoring metabolite fluxes in acetone–butanol–ethanol fermentations, Biotechnol. Bioeng. 99 (2008) 862–869, https://doi.org/10.1002/bit.21639.
[44] S. Junne, M. Nicolas Cruz-Bournazou, A. Angersbach, P. Götz, Electrooptical monitoring of cell polarizability and cell size in aerobic *Escherichia coli* batch cultivations, J. Ind. Microbiol. Biotechnol. 37 (2010) 935–942, https://doi.org/10.1007/s10295-010-0742-5.